Level-Set Segmentation Algorithm

The level-set method, also known as the geometric deformable model, implicitly represents the contour by the zero level of a high-dimensional function called the level-set function $\phi(x, y, t)$. If this contour moves in the normal direction with a speed *F*, then the level set function satisfies the below level set equation,

$$\frac{\partial \phi}{\partial t} + F\left|\nabla \phi\right| = 0$$

where the function *F* is called the speed or energy functional that controls the motion of the contour. This approach has advantages over traditional segmentation methods such as thresholding and region growing, as it has the ability to represent contours with complex topology and to change their topology in a natural way.

In a variation of the level-set formulation, Chan et al. (36) proposed an active contour model using level-set formulation by incorporating region-based information. Assuming *I* is a two-dimensional (2D) image defined on domain Ω, the energy functional that we will minimize is defined as,

$$F^{CV}(\phi, c_1, c_2) = \int_{\Omega} \left|I(\mathbf{x}) - c_1\right|^2 H(\phi(\mathbf{x}))d\mathbf{x} + \int_{\Omega} \left|I(\mathbf{x}) - c_2\right|^2 (1 - H(\phi(\mathbf{x}))d\mathbf{x} + \nu \int_{\Omega} \left|\nabla H(\phi(\mathbf{x}))\right| d\mathbf{x} ,$$

$$H(z)=\begin{cases}1, & \text{if } z\geq 0\\ 0, & \text{if } z<0\end{cases},\qquad \begin{cases}c_1(\phi)=\text{average}(I(\mathbf{x}))\text{ in }\{\phi\geq 0\}=\dfrac{\int_\Omega I(\mathbf{x})H(\phi(\mathbf{x}))d\mathbf{x}}{\int_\Omega H(\phi(\mathbf{x}))d\mathbf{x}}\\ c_2(\phi)=\text{average}(I(\mathbf{x}))\text{n }\{\phi<0\}=\dfrac{\int_\Omega I(\mathbf{x})(1-H(\phi(\mathbf{x})))d\mathbf{x}}{\int_\Omega (1-H(\phi(\mathbf{x})))d\mathbf{x}}.\end{cases}$$

where *H* is the Heaviside function and c_1, c_2 are the average image intensities in the contour, depending on I and ϕ. Image segmentation is achieved by solving to minimize the energy functional F^{CV}.

For the segmentation of more than two regions, Vese et al. (37) proposed a multiphase level-set approach. Theoretically, *N* level sets are used to segment up to 2^N regions. In particular, here we used a two-phase level-set method with the functions denoted as ϕ_1, ϕ_2 and the energy functional as the following,

$$\begin{aligned}F_4^{CV}(\Phi,\mathbf{C})=&\int_\Omega |I(\mathbf{x})-c_{11}|^2 H(\phi_1)H(\phi_2)d\mathbf{x}+\int_\Omega |I(\mathbf{x})-c_{10}|^2 H(\phi_1)(1-H(\phi_2))d\mathbf{x}\\ &+\int_\Omega |I(\mathbf{x})-c_{01}|^2 (1-H(\phi_1))H(\phi_2)d\mathbf{x}+\int_\Omega |I(\mathbf{x})-c_{00}|^2 (1-H(\phi_1))(1-H(\phi_2))d\mathbf{x}.\\ &+\nu\int_\Omega |\nabla H(\phi_1(\mathbf{x}))|d\mathbf{x}+\nu\int_\Omega |\nabla H(\phi_2(\mathbf{x}))|d\mathbf{x},\end{aligned}$$

$$\begin{cases}c_{11}(\phi)=\text{average}(I(\mathbf{x}))\text{ in }\{\phi_1(\mathbf{x})>0,\phi_2(\mathbf{x})>0\},\\ c_{10}(\phi)=\text{average}(I(\mathbf{x}))\text{ in }\{\phi_1(\mathbf{x})>0,\phi_2(\mathbf{x})<0\},\\ c_{01}(\phi)=\text{average}(I(\mathbf{x}))\text{ in }\{\phi_1(\mathbf{x})<0,\phi_2(\mathbf{x})>0\},\\ c_{00}(\phi)=\text{average}(I(\mathbf{x}))\text{ in }\{\phi_1(\mathbf{x})<0,\phi_2(\mathbf{x})<0\}.\end{cases}$$

where $\mathbf{C}=(c_{11},c_{10},c_{01},c_{00})$ is constant vector, and $\Phi=(\phi_1,\phi_2)$ is level set function vector.

However, the Chan-Vese model is based on the assumption of intensity homogeneity. Therefore, local magnetic inhomogeneities and susceptibility effects can cause segmentation errors in MR images. To address the issue of intensity inhomogeneity in MR image segmentation, Li et al. (38) proposed an improved level-set model with a local clustering criterion function. This method describes an image with intensity inhomogeneity, defined as follows:

$$I = bJ + n,$$

where *I* is the observed image, *J* is the true image, *b* is the bias field, and *n* is additive noise. The method is applied in a circular area with a radius ρ centered at each point *y* in the image domain Ω, defined by $O_y \triangleq \{x: |x - y| \leq \rho\}$ Then, each small region is given by:

$$b(\mathbf{x})J(\mathbf{x}) \approx b(\mathbf{y})c_i \quad \text{for} \quad x \in O_y \bigcap \Omega_i \ ,$$

where the constant $b(\boldsymbol{x})c_i$ can be considered to be the approximation of the cluster center within the neighborhood O_y. To estimate $b(\boldsymbol{x})c_i$, the intensities $I(x)$ in the neighborhood O_y are classified into *N* classes. A local intensity criterion function using the K-means clustering method is defined as follows:

$$\varepsilon_y = \sum_{i=1}^{N} \int_{\Omega_i} K(\mathbf{y} - \mathbf{x}) \left| I(\mathbf{x}) - b(\mathbf{y})c_i \right|^2 d\mathbf{x},$$

$$K(u)=\begin{cases}\frac{1}{a}e^{-|u|^2/2\sigma^2}, & \text{for } |u|\le\rho,\\ 0, & \text{otherwise}\end{cases}$$

where $b(\boldsymbol{y})c_i$ are the cluster centers to be optimized, K(y-x) is a nonnegative weighting function, and a is normalization constant such that $\int K(u)=1$. The intensity criterion function is integrated over the entire domain Ω and incorporated into a multi-phase level-set formulation given by:

$$F(\phi,\mathbf{c},b)=\varepsilon(\phi,\mathbf{c},b)+\nu\int|\nabla H(\phi)|d\mathbf{x}+\mu R_p(\phi),$$

$$\varepsilon(\phi,\mathbf{c},b)=\int\sum_{i=1}^{N}\left(\int K(\mathbf{y}-\mathbf{x})|I(\mathbf{x})-b(\mathbf{y})c_i|^2\,d\mathbf{y}\right)M_i(\phi(\mathbf{x}))d\mathbf{x},$$

$$R_p(\phi)=\frac{1}{2}\int p(|\nabla\phi|-1)^2 d\mathbf{x}\ .$$

where $M_1(\phi(\boldsymbol{x}))=H(\phi(\boldsymbol{x}))$ and $M_2(\phi(\boldsymbol{x}))=1-H(\phi(\boldsymbol{x}))$ in the two-phase case. $R_p(\phi)$ is distance regularization term to make level set function smoothly. By minimizing this energy, we obtained the image segmentation result given by the level-set function ϕ and the estimation of the bias field *b*. In this work, we employed this energy model to segment images using the same parameters as in reference (38), μ=0.1, ν=0.001, and σ=4.

Supplemental Figure 1. UTE1 and UTE2 obtained using mMR software versions (A) VB18P and (B) VB20P.

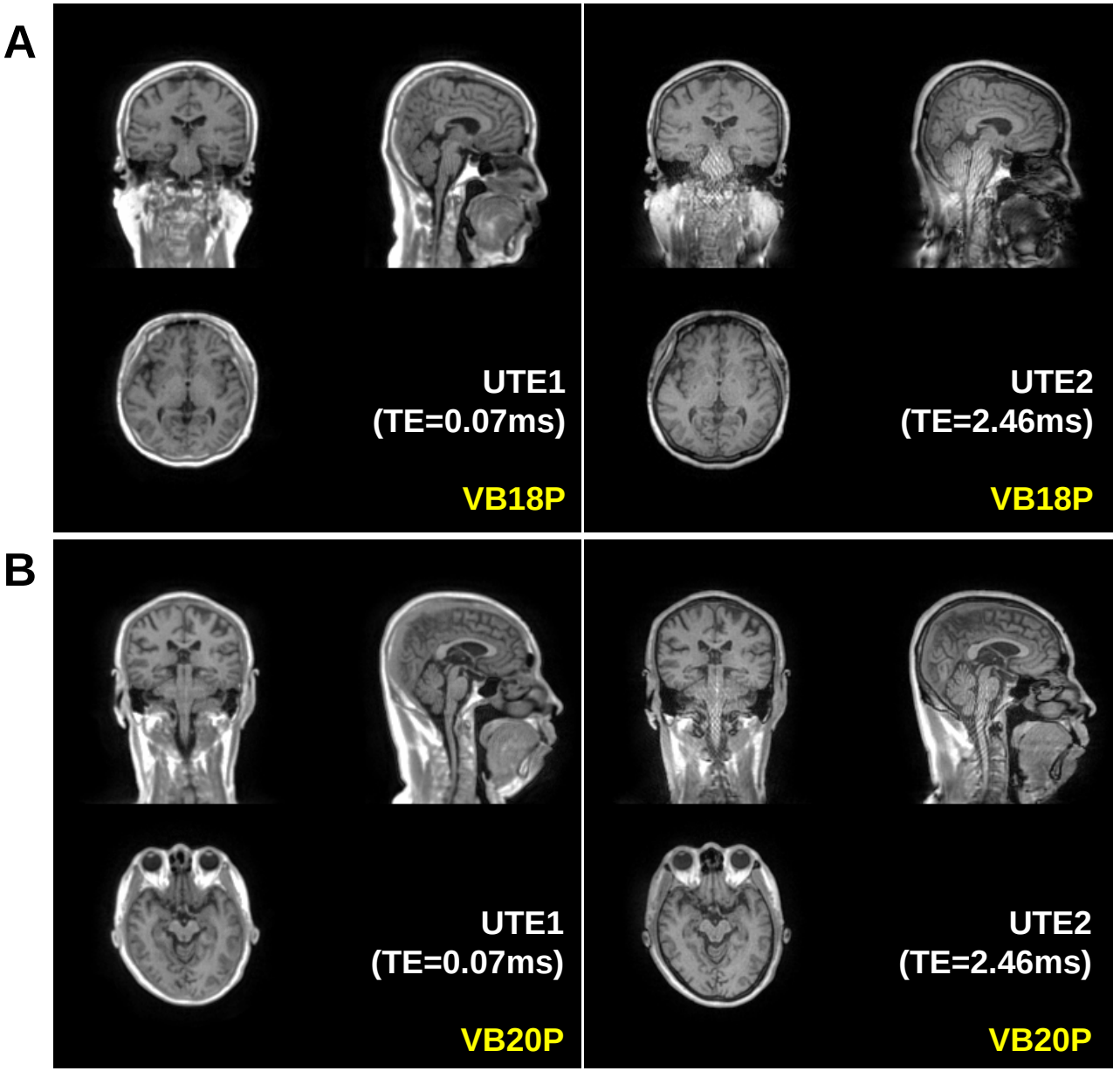

Supplemental Figure 2. Flow chart of PET image generation and analysis.

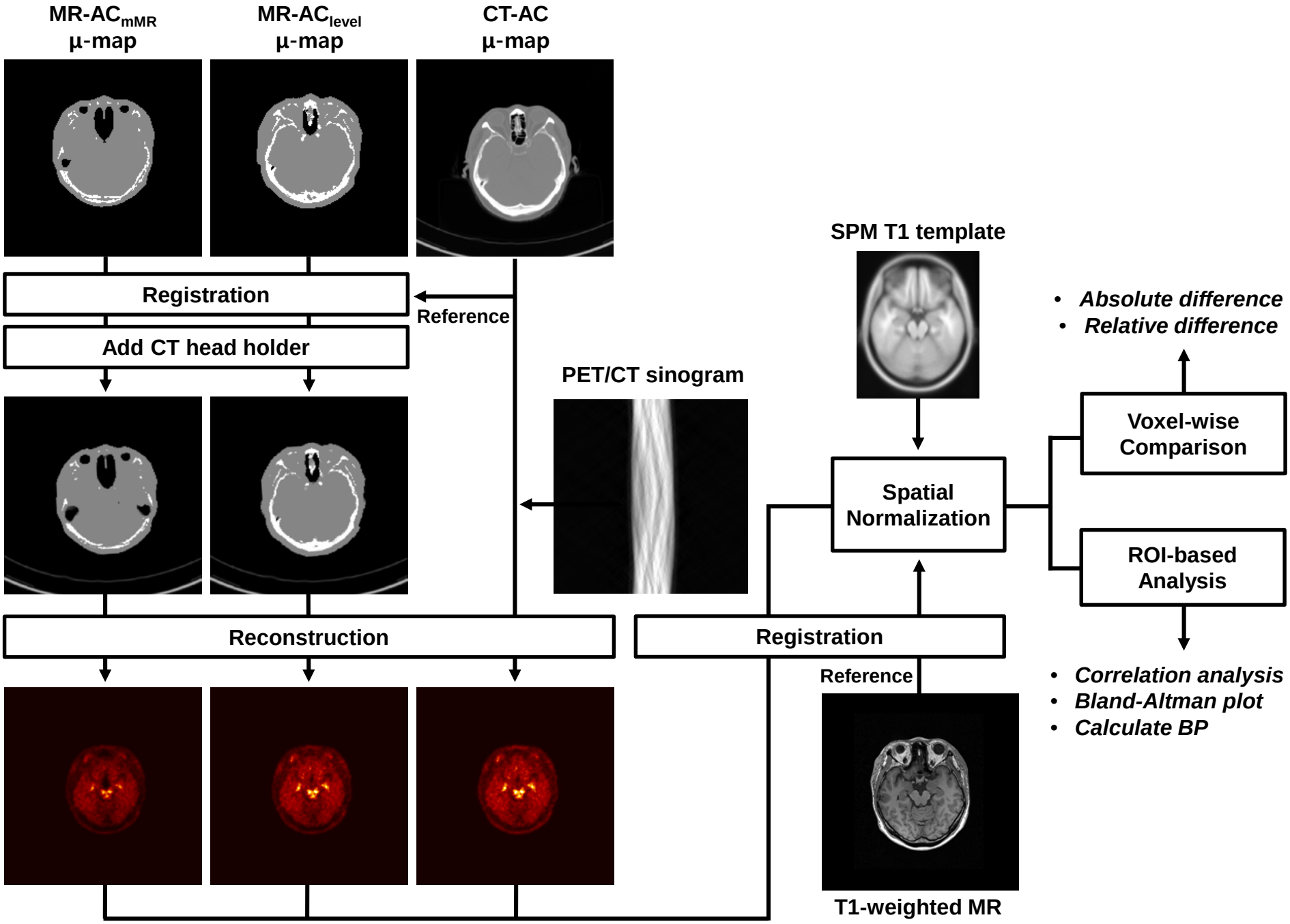

Supplemental Figure 3. SUV (A) and SUVr (B) in each ROI for [^{18}F]FP-CIT PET.

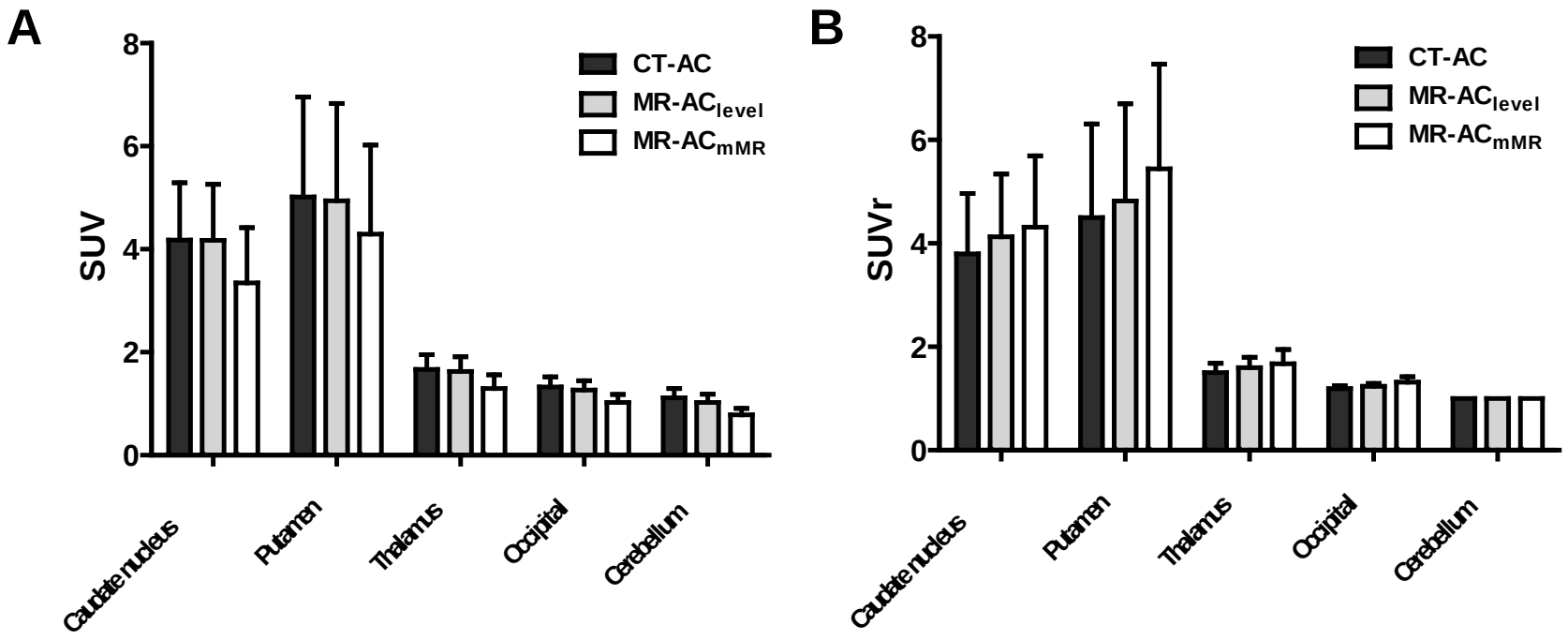

Supplemental Figure 4. Correlation of SUV between CT-AC and (A) MR-AC_{level}, (B) MR-AC_{mMR} in [^{18}F]FP-CIT study.

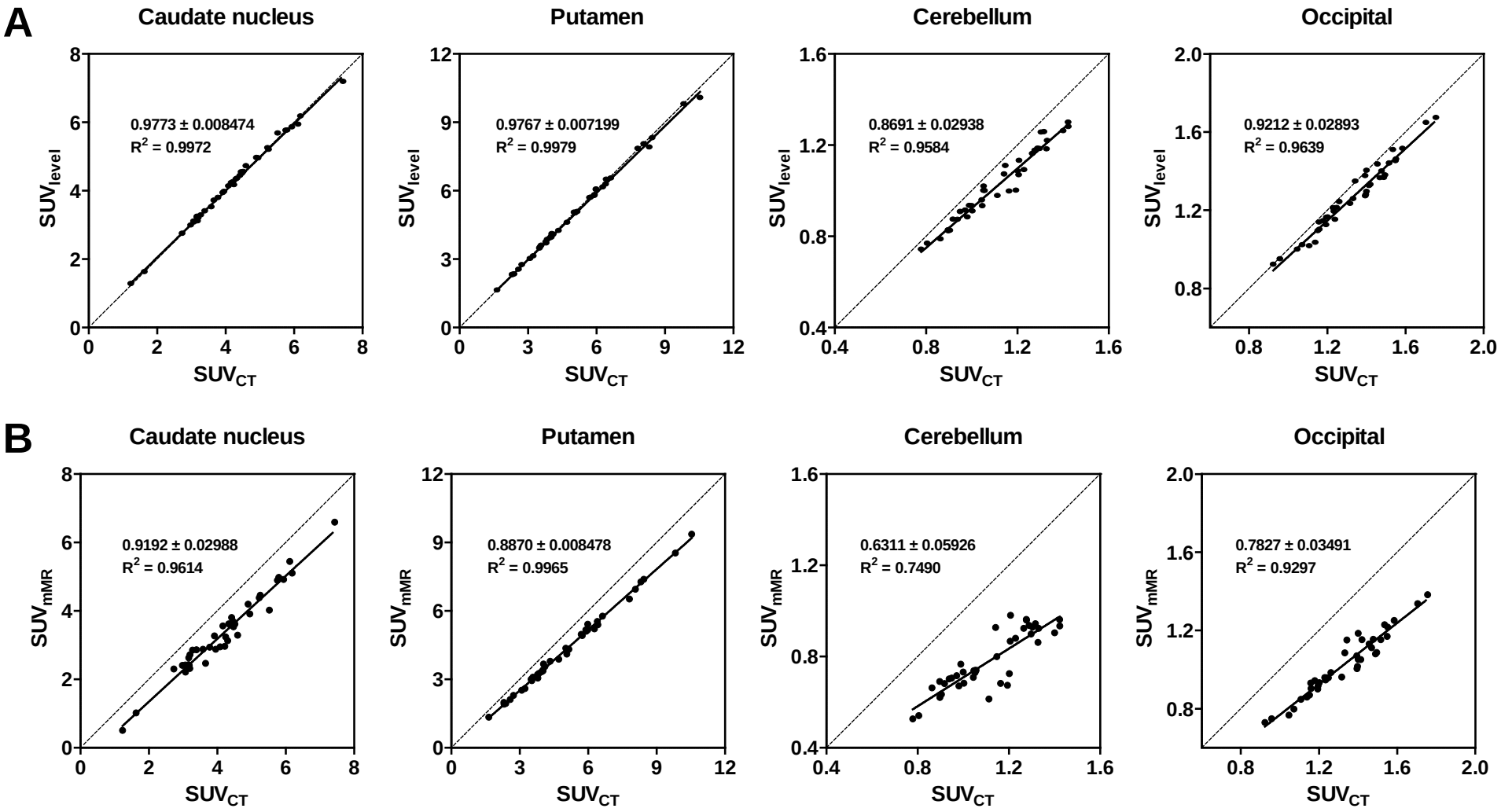

Supplemental Figure 5. Correlation of binding ratio (BR) and Bland–Altman analysis in putamen between CT-AC and (A) MR-AC_{level}, (B) MR-AC_{mMR} in [^{18}F]FP-CIT study.

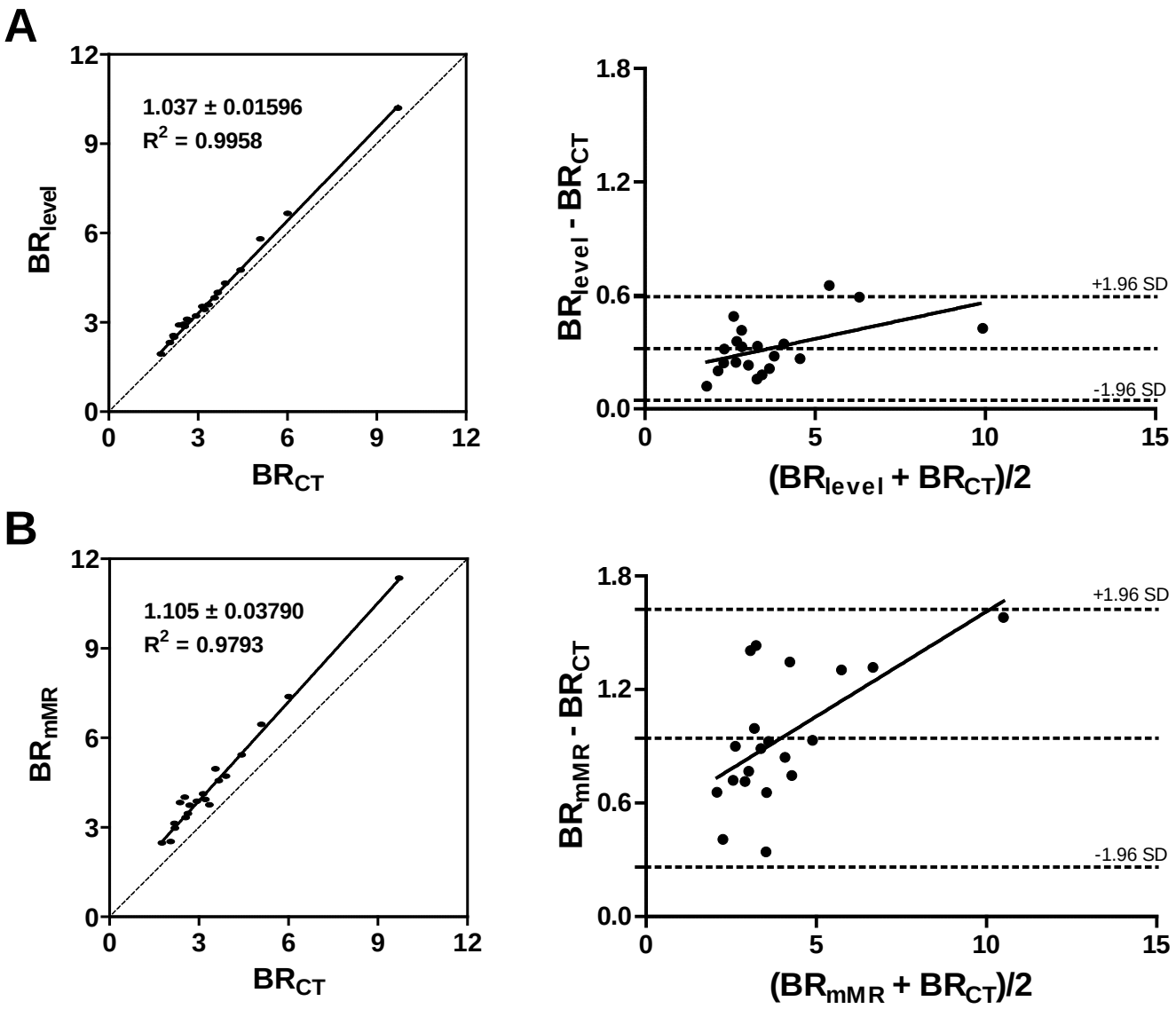

Supplemental Figure 6. Correlation of binding ratio (BR) and Bland–Altman analysis in caudate nucleus between CT-AC and (A) MR-AC_{level}, (B) MR-AC_{mMR} in [^{18}F]FP-CIT study.

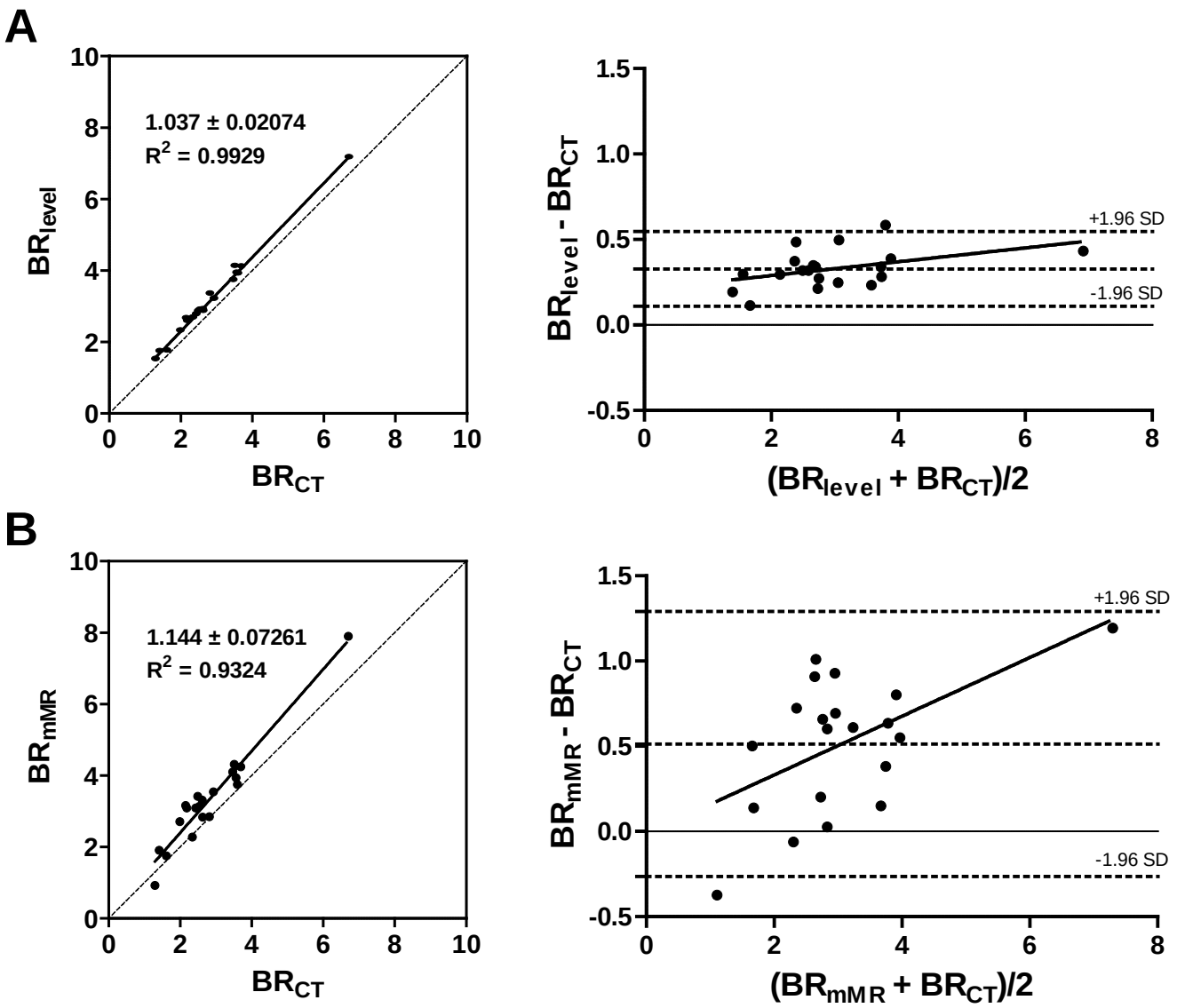

Supplemental Figure 7. SUV (A) and SUVr (B) in each ROI for [^{18}F]FDG PET.

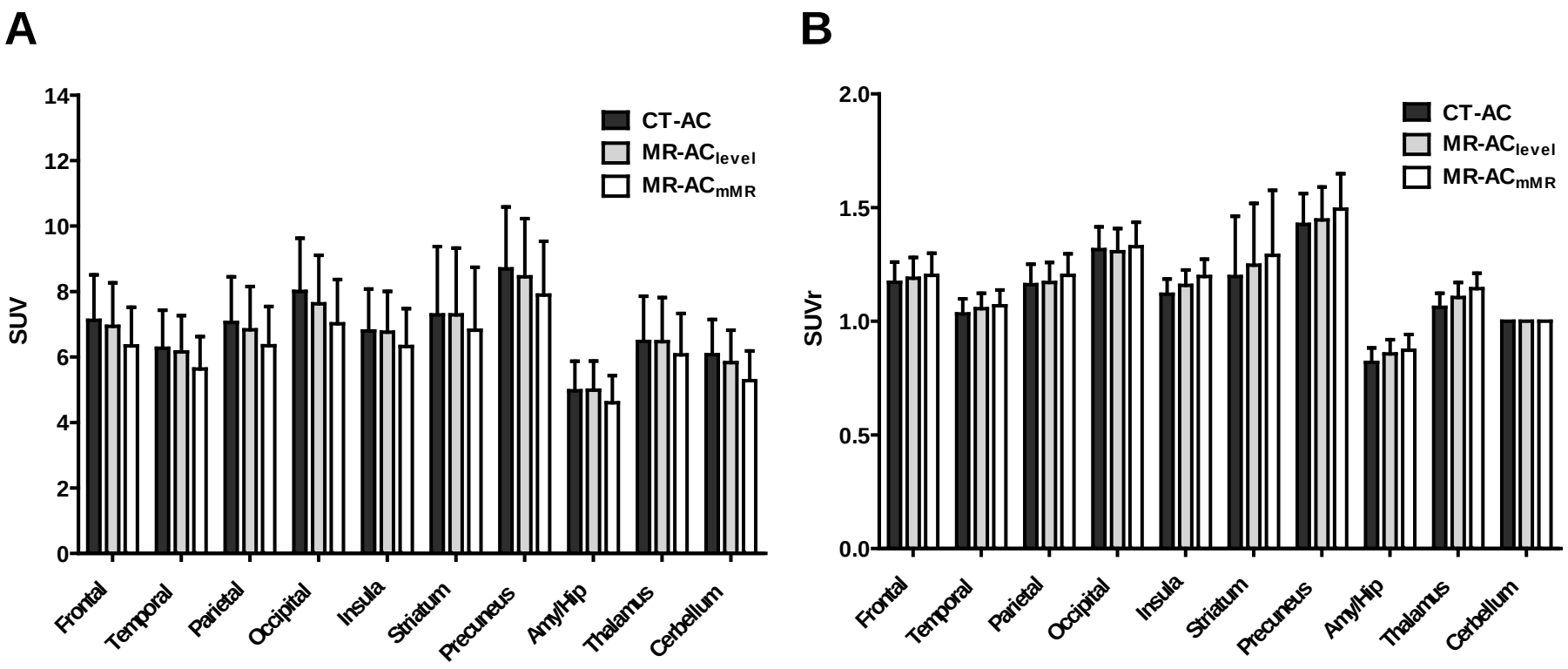

Supplemental Figure 8. Correlation of SUV and Bland–Altman analysis in whole brain between CT-AC and (A) MR-AC_{level}, (B) MR-AC_{mMR} in [^{18}F]FDG study.

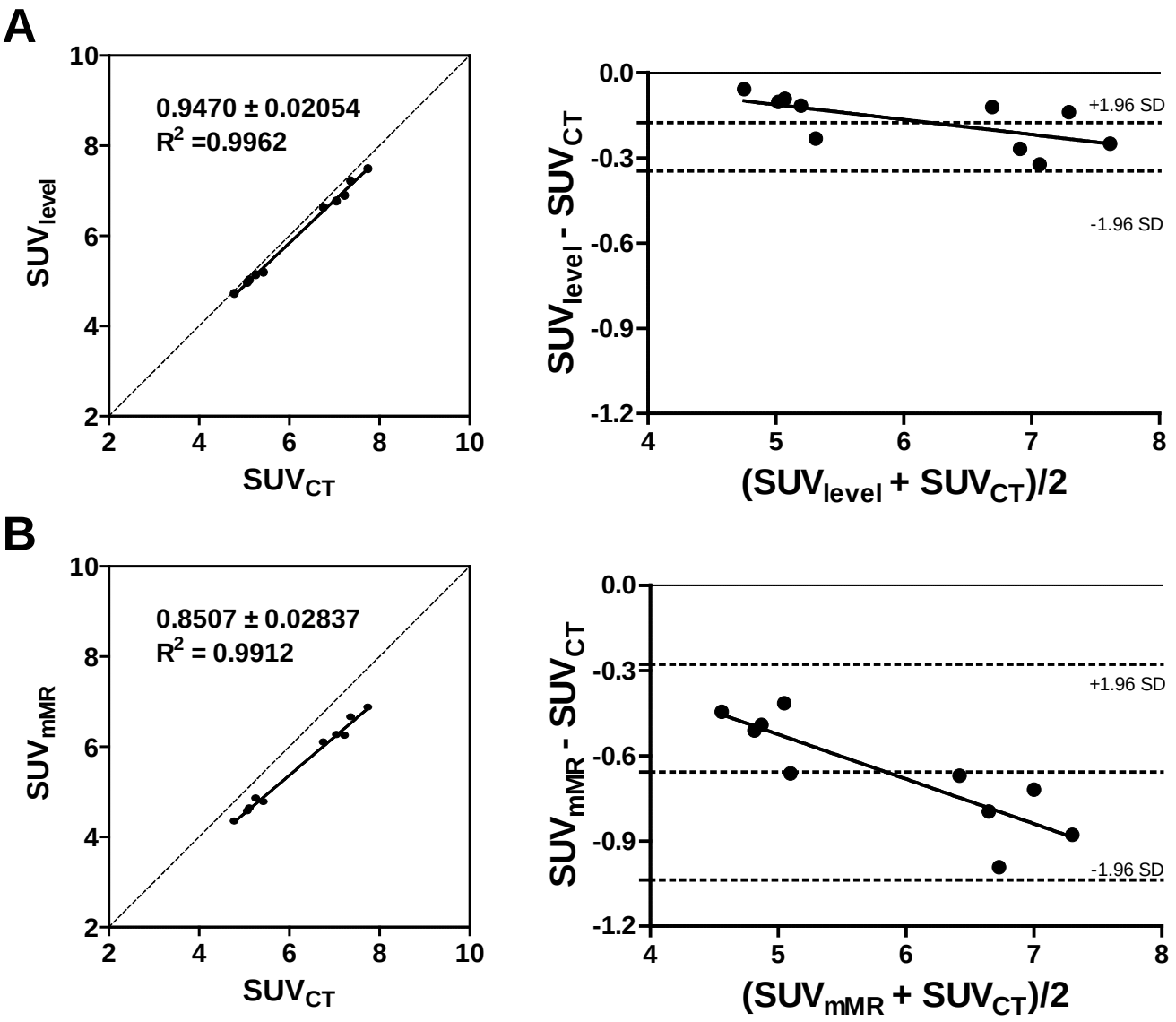

Supplemental Figure 9. Correlation of SUV and Bland–Altman analysis in cerebellum between CT-AC and (A) MR-AC_{level}, (B) MR-AC_{mMR} in [^{18}F]FDG study.